Research on the Impact Resistance of the Periodic Helicoidal Multilayer Bionic Structure Based on Osteon Microstructure

Yuxi Liu (yuxiliu66@126.com)
Chongqing University
Ai-hua Li
Chongqing University Cancer Hospital
Bin Chen
Chongqing University
Yan-hua Li
Children's Hospital of Chongqing Medical University

Research

Keywords: osteon, lamella, mineralized fibril, periodic helicoidal structure, impact resistance, bionic composite

Posted Date: April 6th, 2021

DOI: https://doi.org/10.21203/rs.3.rs-354443/v1

Research on the impact resistance of the periodic helicoidal multilayer bionic structure based on osteon microstructure

Yu-xi Liu[a,c*], Ai-hua Li[b], Bin Chen[c], Yan-hua Li[d*]

[1] College of Mechanical Engineering, Chongqing Vocational Institute of Engineering, Chongqing 402260, China

[2] Key Laboratory for Biorheological Science and Technology of Ministry of Education, Chongqing University Cancer Hospital, Chongqing 400030, China

[3] College of Aerospace Engineering, Chongqing University, Chongqing 400044, China

[4] Ministry of Education Key Laboratory of Child Development and Disorders, China International Science and Technology Cooperation base of Child development and Critical Disorders, Children's Hospital of Chongqing Medical University, Chongqing 400014, China

Abstract:

Background: As a typical biological material, bone have excellent mechanical properties and plays an important role in supporting the animal body and protecting organs, osteon is an important part of bone. It is found that the osteon is composed of thin and thick lamellae which are periodic and approximately concentric, every 5 lamellae is a cycle, the periodic helix angle of mineralized collagen fibers in two adjacent sub-lamellae is 30°. Four biomimetic composite models with different fiber helix angles were established and fabricated according to the microstructure of mineralized collagen fibers in osteon. Based on the impact analysis of four kinds of bionic composite models, the effects of the fiber periodic helicoidal structure on the impact resistance and energy dissipation of multi-layer bionic composite were investigated.

Results: The analysis results show that the fiber helix angle affects the impact damage resistance and energy dissipation of multi-layer fiber reinforced composites. Among the four kinds of multi-layer composite models, the composite model with helix angle of 30° has better comprehensive ability to resist impact damage. The test results show that the impact damage area of the specimen with 30° helix angle is smallest among the four types of bionic specimens, which is consistent with the results of finite element impact analysis. Furthermore, in the case of no impact damage, the smaller the fiber helix angle is, the more uniform the stress distribution is and more energy is dissipated in the impact process.

Conclusions: The periodic helicoidal structure of mineralized collagen fibers in osteon are the result of natural selection of biological evolution. This structure can effectively improve the ability of cortical bone to resist external impact. The research results can provide useful guidance for the design and manufacture of high-performance and strong impact resistant biomimetic composites.

Keywords： osteon, lamella; mineralized fibril; periodic helicoidal structure; impact resistance; bionic composite

Background

*Corresponding author: yuxiliu66@126.com (Y. Liu); huahua062883@sohu.com (Y. Li).

After hundreds of million-year of natural evolution, the unique biological structure of animals and plants have excellent mechanical properties which can achieve self-protection or resist natural enemies [1-7]. With the rapid development of modern science and technology, composite materials with high strength, light weight and impact resistance have a wide range of needs in the fields of aerospace, military, automobiles and other fields. Thus, the investigation of biomimetic composite materials can provide enlightenment for the design of exceptional impact resistant material and meet special requirement of engineering [8-10].

As a typical biological material, bone plays an important role in supporting the animal body and protecting organs, which is composed of cortical bone and cancellous bone. From a structural viewpoint, cortical bone tissue can be considered as a composite material hierarchically structured at different scales. At the microscale, the mineralized collagen fibrils are grouped together in a certain direction to form lamellar structure, and the thickness is about of 3-7μm. Further, these lamellae are concentrical surround the haversian canal to compose osteons [11] and its diameter ranges from 50 to 500μm [12]. At the nanoscale, cortical bone is mainly composed of organic phase [13] and inorganic phase, the organic phase is mainly formed by mineralized collagen fibrils [14]. Mineralized collagen fibers are ubiquitous in various biological materials and are mainly arranged helicoidally [15], and there are extensive researches on multilayer fiber bionic composite [16-17]. However, the mineralized collagen fibers in osteons have their own uniqueness, which are periodic helicoidal arranged and every 5 sub-lamellae constitute a lamella. The arrangement of mineralized collagen fibers in adjacent sub-lamellae is shown in Fig.1(a) [18-19], the five directions represent the fiber directions in five consecutive sub-lamellae in each lamella and the helicoidal angle of two adjacent fibers is 30°.Giner et al. [11] drew a schematic diagram of the staggered structure of sub-lamellae of osteons and the fiber directions of the five sub-lamellae (Fig. 1(b)), and the 5 sub-layers are simplified to a thin layer and a thick layer [20].

At present, the research on osteons mainly focuses on the microstructure of osteons [21-23], distribution of collagen fibers and osteocyte lacunae [24-25]. However, there is no report on the biomimetic composite material with periodic helicoidal arrangement of fibers based on osteon. In this paper, the biomimetic composite material models with periodic helicoidal structure were investigated based on the arrangement of fiber in osteon. Four bionic composite models were constructed and fabricated for comparing and analyzing the effect of the periodic helicoidal arrangement structure of fibers on the impact characteristics of composite. Then, low-velocity impact damage analysis and drop weight test were performed, the finite element (FE) analysis is based on Hashin failure criterion and progressive damage analysis method, the influence of fiber layup method on the impact damage and energy dissipation ability of biomimetic composites were investigated.

Results

Effects of laying mode on damage resistance

When the multi-layer composites with different fiber arrangement are subjected to external impact, the in-plane damage is quite different. In order to compare and analyze the impact of different fiber stacking methods on the impact characteristics, the same boundary conditions were used for the four models in the impact analysis process, that is, the impact load and boundary constraints are the same.

(1) Fiber compression failure

When the impact energy is 20J, the initial failure of fiber compression and the failure distribution

nephogram of the four kinds of bionic composite models in the impact process are shown in Fig.2 and Fig.3, respectively. According to the previous analysis of fiber compression failure criterion, the fiber compression failure occurs when the failure criterion is equal to 1, the fiber compression failure occurs when the failure criterion is greater than 1. It can be seen from the analysis results (Fig.2) that with the increase of impact energy, the fiber compression failure occurs first in the orthogonal material model (sample 90), followed by the sample 30 model, and finally the sample 15 model. However, there is no obvious fiber compression failure in the sample 60 model under the impact load. In addition, it can be seen from Fig.2 that although the fiber compression failure exists in the sample 15, sample 30 and sample 90 models, there is a significant difference in the failure initiation time.

In the distribution nephogram of fiber compression failure, the red area represents the part of fiber compression failure. It can be seen from the failure distribution nephogram (Fig. 3) that the fiber compression failure ratio in the sample90 model is the largest, followed by the sample15 model, and the failure proportion in the sample30 model is the smallest, which indicates that the collagen fiber arrangement structure with a helicoidal angle of 30° is helpful to enhance the compression resistance ability of osteon.

The above analysis results show that the fiber stacking mode directly affects the compression failure of the fiber. By adjusting the fiber stacking mode in the multi-layer composite, the initial time of fiber compression failure and the ratio of fiber compression failure can be effectively improved.

(2) Fiber tensile failure

Fig.4 shows the time history of fiber tensile initial failure of four bionic composite models during impact process. It can be seen from the analysis results that under the same impact load, the model of sample90 first appears fiber tensile failure. The second model is sample60 and sample30, but there are some differences in their time histories. Finally, the sample15 model, and the fiber tensile failure time of sample15 is much later than the first three models, which shows that the fiber has strong ability to resist tensile crack initiation in sample 15. Followed by the sample60 and sample30 models, but there are also certain differences in their time history. Finally, the sample15 model, and the fiber tensile failure time of sample 15 is much later than the first three models, which shows that the fiber has strong ability to resist tensile crack initiation in model sample15.

It can be seen from the distribution nephogram of fiber tensile failure (Fig.5) that the proportion of fiber tensile failure increases in three models with fiber helix angle from 30° to 90°. However, the fiber tensile failure ratio is the largest when the helix angle is 15°, which indicates that the smaller the helix angle, the stress of the fiber in the model is more uniform. Once the failure occurs, the damage ratio will increase rapidly. The above analysis results show that the tensile strength of the multi-layer composite with fiber helix angle of 30° is stronger. Simultaneously, it also shows that the helicoidal structure of collagen fibers with a helix angle of 30º in osteon helps to enhance the tensile strength of cortical bone.

(3) Matrix compression failure

Under the load of 20J impact energy, the matrix compression failure history with time is shown in Fig.6. It can be seen from Fig.6 that matrix compression failure occurs first in sample30 and sample60, followed by sample15, and finally by sample90. Fig.7 shows the matrix compression failure distribution nephogram of the four models at the end of the impact. From the analysis results, it can be seen that although sample90 is the last matrix compression failure, the failure area is the

largest at the end of the impact. In addition, by comparing the failure nephogram of the four models, it can be seen that the failure ratio of sample15 and sample90 is larger, while that of sample30 and sample60 are smaller. The results show that the stacking mode also affects the matrix compression failure for multi-layer fiber reinforced composites. Furthermore, when the multi-layer fiber reinforced composites are subjected to external impact, too large or too small fiber helix angle is not conducive to resistance compression failure of matrix.

(4) Tensile failure of matrix

According to the impact damage analysis results of the four models, it can be seen that the matrix tensile failure is the first to occur in the four models. When the impact energy is 20J, the matrix tensile failure distribution of the four models is shown in Fig. 8. Because the mechanical properties of the matrix in the multi-layer fiber reinforced composites are much lower than that of the reinforced phase, the matrix is usually damaged first when it is subjected to external force, so the analysis results in this section are consistent with the actual situation. In addition, according to the matrix tensile failure distribution nephogram of the four models, it can be seen that the matrix compression failure distribution nephograms of sample30, sample60 and sample90 are similar, but the tensile failure areas of the matrix are not different. Compared with the other three models, the tensile failure area of the matrix in sample15 is the smallest, and the failure distribution nephogram is obviously different from the other three models. The analysis results show that under the same material composition, boundary conditions and impact load, the fiber layering method also affects the tensile failure of the matrix, and the small fiber helix angle can make the matrix stress distribution more uniform, which is helpful to enhance the tensile strength of the matrix.

Effects of laying mode on energy dissipation

Energy is an important factor in low speed impact test. The difference between the impact energy and the kinetic energy of punch pin at the end of the impact is defined as the energy dissipated by the composite plate during the impact. The "dissipated energy" defined here also includes other energy consumption during impact process, such as strain energy released by sandwich plate, kinetic energy of sandwich plate, strain energy released by punch, consumption of viscous damping and friction. The energy is difficult to accurately count and is very small, so it can be ignored. In addition, compared with multilayer composite materials, the punch is regarded as a rigid body, and its strain energy can also be ignored. In addition, compared with the multilayer composite, the punch is regarded as a rigid body, and its strain energy can be ignored.

The calculation method of impact energy used in this paper as follows: the kinetic energy of the punch at the moment of contact is regarded as the impact energy. Therefore, the actual impact energy E_{impact} and the dissipated energy of composite plate $E_{dissipated}$ are defined as follows:

$$E_{\text{impact}} = \frac{1}{2} m v_0^2 \tag{1}$$

$$E_{\text{dissipated}} = \frac{1}{2} m v_0^2 - \frac{1}{2} m v_t^2 \tag{2}$$

where, m is the mass of the punch, in this study m = 2kg (the mass of different sizes of punch is slightly different in actual experiment); g is the acceleration of gravity; h is the distance of the punch relative to the upper surface of the test model before release; v_0 and v_t are the velocities of the punch at the moment of contact and separation between the punch and the upper surface of the model, respectively.

When the impact energy is 20J, the kinetic energy change history of the four models is shown in

Fig. 9. It can be seen from Fig. 9 that when the punch contacts with the composite plate, the velocity gradually decreases to zero, and then it is ejected and detached from the composite plate. The kinetic energy when the punch separates from the plate is the residual energy of impact. According to the kinetic energy change curve in Fig. 9, the energy dissipated by the four models in the impact process is shown in Fig.10.

It can be seen from Fig. 10 that when the helix angle of the fiber decreases from 60° to 15°, the energy dissipated increases by 5.94% for sample30 and 18.37% for sample15 compared with sample60.The energy dissipated by the Sample90 model is the largest. According to the above analysis of the four models can be known, this is due to more matrix and fiber damage in the sample90.

Bionic specimens test results

Fig. 11 shows the failure mode of layered bionic specimens after impact. It can be seen from Fig. 11 that bionic composite laminates with different helix angles have varying degrees of damage under the same impact load. The results show that the impact damage area of the sample with 30° helix angle is smallest among the four types of bionic specimens. It can be concluded that the bionic composite laminate with fiber helix angle of 30° has a better ability to resist impact damage, which is consistent with the results of finite element impact analysis, which also shows the correctness of the FE analysis.

Conclusions

In order to investigate the effect of fiber periodic helix ply structure on the impact resistance of multilayer composites, four kinds of bionic composite models with different fiber helix angles were established according to the microstructure characteristics of osteon, and the progressive damage analysis method and Hashin failure criterion were used to study the impact damage and energy dissipation capacity of the four models. Then, the bionic structure with different helix angles were fabricated and tested. The conclusions are described as follows:

(1) The impact resistance of multi-layer fiber reinforced composites is affected by the way of fiber arrangement. The analysis results show that among the four bionic composite models with fiber helix angles of 15º, 30º, 60º and 90º, the model with a fiber helix angle of 30° has the best comprehensive ability to resist impact damage.

(2) The smaller fiber helix angle can make the matrix stress distribution more uniform, which is helpful to enhance the tensile failure resistance of matrix. The impact analysis results show that the tensile failure area of the matrix in sample15 is the smallest under the same boundary conditions and impact load.

(3) The size of the fiber helix angle affects the energy dissipation capacity of the multilayer fiber reinforced composite. In the case of no impact damage, the smaller the fiber helix angle, the more energy dissipated in impact process.

(4) The test results show that the impact damage area of the specimen with 30° helix angle is smallest among the four types of bionic specimens and has a better ability to resist impact damage, which is consistent with the results of finite element impact analysis.

(5) The helical structure of mineralized collagen fibers in osteon is the result of natural selection of biological evolution. This structure can effectively improve the ability of cortical bone to resist

external impact. The research results can provide useful guidance for the development of high-performance bionic composite materials.

Methods

Bionic design and impact analysis

According to the helicoidal structure of mineralized collagen fiber in osteon, a bionic composite model of periodic helicoidal structure model with the fiber helix angle increasing by 30º was constructed (Tab.1, Sample 30). In addition, in order to compare and analyze the effects of fiber helix angle on the impact resistance of biomimetic composites, a composite material model of osteon-like with 0º/90º orthogonal model and fiber helix angle of 15º and 60ºmodels were constructed (Table 1). Then, the effects of different fiber arrangement structure on the impact resistance and energy dissipation capacity of the bionic composite were investigated based on finite element (FE) analysis method.

It is assumed that the thickness of each sublayer in the helicoidal structure is same and the layers are well integrated among themselves. Then, according to the periodic helicoidal arrangement structure of the fibers in osteon, a 12-layer periodic helicoidal arrangement structure bionic model was constructed in ABAQUS (Fig.12). The geometric size of the model is 150mm× 100mm×6mm (standard thickness in ASTM-D-7136: 4~6 mm), and the single layer thickness is 0.5 mm. The thickness of biomimetic composite material model is 6 mm in Table 1, and the thickness of each sublayer is equally distributed. The mechanical performance parameters of the composite material models used in FE analysis are shown in Table 2 [26-27].

The impact analysis was performed on the four bionic material models using drop-weight impact testing. In the analysis process, the impact energy of 20J was selected, the mass of the drop-weight is 2kg, and the critical contact velocity is 4.47 m/s. The elastic modulus E and Poisson's ratio v of the punch are 210 GPa and 0.3 respectively. The deformation of the punch is ignored in the process of impact analysis, that is, the punch is constrained as a rigid body. The shape of the punch tip is hemispherical with a diameter of ϕ16 mm. A reference point was chosen on the punch and added a mass point. Impact velocity was applied on the mass point, that is, the impact energy is applied to the punch according to the formula $E=mv^2/2$. Then, the impact responses of four material models were studied under the same impact energy.

The impact analysis model of periodic helicoidal bionic structure with fiber helix angle of 30°is shown in Fig.12a, the local enlarged view of the model and the arrangement direction of the fibers in each layer are shown in Fig.12b-c. For multi-layer composite structure analysis, the 3D shell element model can not only save the calculation cost, but also obtain higher accuracy. Therefore, the four models constructed in this analysis are modeled by 3D shell element, and the element type and size are the same. In addition, due to the severe mesh deformation in impact center area, in order to improve the calculation accuracy, the mesh in the impact center area was refined in the meshing stage. Then the mesh size is transferred to the boundary region in order to ensure the mesh quality and reduce the calculation time.

There are 6 292 nodes and 6 275 hyperbolic shell elements (S4R) with large strain, reduced integral and sand leakage control. According to the specimen requirements of ASTM- D-7136 for drop-weight impact test, full restraint was applied to the four sides of the model. Due to the hard contact between the punch and the composite plate in impact process which will cause the failure of contact element. So the ordinary hard contact algorithm is adopted. During the impact process of

the model, the failure degradation of the element is based on the Hashin failure criterion, and the fiber is 0º along the 1 direction and 90º along the 2 direction (Fig. 12a).

Material failure criterion of impact analysis

There are many kinds of damage in multi-layer composite under low-speed impact load, which are mainly divided into in-plane damage and interlayer damage. The in-plane damage of composites mainly includes fiber fracture and matrix crack, and the interlaminar damage mainly refers to delamination failure between sublayers. Because the material is squeezed under impact load, the local interlaminar damage will not cause complete damage of the material. Therefore, this paper focuses on the comparison and analysis of the in-layer damage of materials with different fiber stacking methods.

Damage failure criterion The Hashin criterion is used to simulate the impact damage of multilayer composite, which can predict the in-plane damage process of multilayer composite, including fiber tensile failure, fiber compression failure, matrix tensile failure and matrix compression failure. Due to the Hashin failure criterion can accurately determine various damage failure modes and is simple and effective, it has been widely used in practice. The combination of Hashin failure criterion and stiffness degradation criterion can simulate the progressive damage process of composite materials and can be easily realized.

The expression of Hashin failure criterion is as follows:

Fiber tensile failure ($\sigma_{11} \geq 0$)

$$\left(\frac{\sigma_{11}}{X^T}\right)^2 + \left(\frac{\sigma_{12}}{S^L}\right)^2 = 1 \tag{3}$$

Fiber compression failure ($\sigma_{11} < 0$)

$$\left(\frac{\sigma_{11}}{X^C}\right)^2 = 1 \tag{4}$$

Tensile failure of matrix ($\sigma_{22} \geq 0$)

$$\left(\frac{\sigma_{22}}{Y^T}\right)^2 + \left(\frac{\sigma_{12}}{S^L}\right)^2 = 1 \tag{5}$$

Matrix compression failure ($\sigma_{22} < 0$)

$$\left(\frac{\sigma_{22}}{2S^T}\right)^2 + \left[\left(\frac{Y^C}{2S^T}\right)^2 - 1\right] \cdot \left(\frac{\sigma_{22}}{Y^C}\right) + \left(\frac{\tau_{12}}{S^L}\right)^2 = 1 \tag{6}$$

where, X^T is the longitudinal tensile strength of the single layer; X^C is the longitudinal compressive strength of the single layer; Y^T is the transverse tensile strength of the single layer; Y^C is the transverse compressive strength; S^L is the longitudinal shear strength; S^T is the transverse shear strength; σ_{11}, σ_{22} and τ_{12} are effective stress tensor components.

Material degradation criterion Material degradation (i.e. material stiffness degradation) means that when the element satisfies certain failure criteria in the finite element model, the elements in

the model will be damaged (including matrix failure, fiber failure and delamination). According to these different damage modes, the material properties of the damage element in the model need to be given new values according to certain rules, so as to obtain a new material model.

In the finite element progressive damage analysis, there are many methods to degrade the stiffness of the element. In this research, the material parameter degradation mode [28] proposed by Tan was used to degrade the stiffness of damaged area, and different in-plane damage modes correspond to different degradation schemes, as shown in Table 3.

Bionic composite fabrication and test

Specimen fabrication According to the designed four kinds of fiber periodic spiral structure models, unidirectional glass fiber prepreg (glass fiber / epoxy resin, model: G 12500) was used to fabricate bionic spiral structure composite laminates. The fiber ratio of unidirectional glass fiber prepreg is 125g/m^2, the resin content is 33% (included 33 wt% - of resin), and the thickness of single layer is 0.1 mm. The fabrication processes of the composite laminate with fiber periodic helix ply structure are as follows:

(1) The prepreg was cut into a square of 120mm×120mm.

(2) The cut prepreg was rotated periodically at the angles of 15°, 30°, 60° and 90° (Fig.13). The number of layers is 12.

(3) The prepreg lamination is put into the hot press mold, and the hot press (hot press model: hy61zf) is used for hot press curing.

The hot pressing process is as follows:

(1) The initial pressure is 2t, and the temperature is raised to 200℃;

(2) After holding the pressure for 5 minutes, the pressure dropped to 1t;

(3) The composite laminate with bionic spiral structure can be obtained by keeping the pressure for 120 minutes and cooling naturally.

Drop weight test The composite laminates with bionic spiral ply structure were made into drop weight impact test specimens (size: 50mm × 50mm). Then, the tests were conducted according to the test method of ASTM- D-7136 for drop-weight impact test. The model of impact testing machine is XH-2000, and the diameter of rigid body punch is 8.5mm, the mass of the drop-weight is 2kg, the drop height is 1m. The total impact energy (J) of a specimen was computed by the equation $E = MgH$, where M is the weight of the hammer (kg), g is 9.8 m/s^2, and H is the height of drop weight (m).

Acknowledgments

Not applicable.

Authors' contributions

The authors prepared the whole manuscript.

Funding

This work was supported by the Chongqing Research program of Basic Research and Frontier Technology (Grant No. cstc2018jcyjAX0805), and the Science and Technology Research Program of Chongqing Municipal Education Commission (Grant No. KJQN201903407).

Availability of data and materials

The data and material will be available on request.

Ethics approval and consent to participate

This article does not contain any studies with human participants or animals performed by the authors.

Consent for publication

This research has no limitation for publication.

Conflicts of interest

The authors declare no conflicts of interest.

References

1. Tsang HH, Raza S. Impact energy absorption of bio-inspired tubular sections withstructural hierarchy. Compos Struct, 2018; 195: 199–210.
2. Sabah SHA, Kueh ABH, Al-Fasih MY. Comparative low-velocity impact behavior ofbio-inspired and conventional sandwich composite beams. Compos Sci Technol. 2017;149: 64–74.
3. Xiang J, Du J, Li D, Scarpa F. Numerical analysis of the impact resistance in aluminum alloy bi-tubular thin-walled structures designs inspired by beetle elytra. J Mater Sci. 2017;52(22): 13247–60.
4. Yin H, Huang X, Scarpa F, Wen G, Chen Y, Zhang C. In-plane crashworthiness of bioinspired hierarchical honeycombs. Compos Struct. 2018;192: 516–27.
5. Jiang H, Ren Y, Liu Z, Zhang S. Microscale finite element analysis for predicting effects of air voids on mechanical properties of single fiber bundle in composites. J Mater Sci. 2019;54(2): 1363–81.
6. Jopek H, Strek T. Torsion of a two-phased composite bar with helical distribution ofconstituents. Phys Status Solidi, 2017;254(12): 1700050.
7. Bhudolia SK, Joshi SC. Low-velocity impact response of carbon fibre composites with novel liquid Methylmethacrylate thermoplastic matrix. Compos Struct, 2018; 203: 696–708.
8. Ballarini R, Heuer AH. Secrets in the shell: the body armor of the queen conch is much tougher than comparable synthetic materials. What secrets does it hold? Am. Sci. 2007;95(5): 422-9.
9. Naleway SE, Porter MM, McKittrick J, Meyers MA. Structural design elements in biological materials: application to bioinspiration. Adv Mater, 2015; 27(37): 5455-76.
10. Chen PY, Mckittrick J, Meyers MA. Biological materials: functional adaptations and bioinspired designs. Prog Mater Sci, 2012; 57(8): 1492-704.
11. Giner E, Arango C, Vercher A., Javier-Fuenmayor F. Numerical modelling of the mechanical behaviour of an osteon with microcracks. J. Mech. Behav. Biomed. Mater. 2014; 37: 109-124.
12. Currey JD. The structure and mechanics of bone. J. Mater. Sci. 2012; 47: 41-54.
13. Dunlop JWC, Fratzl P. Biological composites. Annu Rev Mater Res, 2010; 40: 1-24.
14. Hamed E, Lee Y, Jasiuk I. Multiscale modeling of elastic properties of cortical bone. Acta. Mech. 2010; 213: 131-154.
15. Wang Z, Sun Y, Wu H, Zhang C. Low velocity impact resistance of bio-inspired building ceramic composites with nacre-like structure. Construction and Building Materials, 2018;169: 851–858.
16. Wei Z, Xu X. FEM simulation on impact resistance of surface gradient and periodic layered bionic composites. Composite Structures, 2020; 247: 112428.
17. Jiang H, Ren Y, Liu Z, Zhang S, Lin Z. Low-velocity impact resistance behaviors of bio-inspired helicoidal composite laminates with non-linear rotation angle based layups.

Composite Structures, 2019;214: 463-475.
18. Giraudguille MM. Twisted plywood architecture of collagen fibrils in human compact bone osteons. Calcif Tissue Int. 1988; 42(3): 167-80.
19. Liu D, Wagner HD, Weiner S. Bending and fracture of compact circumferential and osteonal lamellar bone of the baboon tibia. J Mater Sci: Mater Med, 2000;11(11):49-60.
20. Vercher A, Giner C, Arango C. Homogenized stiffness matrices for mineralized collagen fibrils and lamellar bone using unit cell finite element models. Biomech Model Mechanobiol, 2014;13(2): 437-449.
21. Barth HD, Zimmermann EA, Schaible E, Tang SY, Alliston T. Characterization of the effects of x-ray irradiation on the hierarchical structure and mechanical properties of human cortical bone. Biomaterials, 2011; 32(34): 8892-8904.
22. Vercher-Martínez. A,Giner E, Arango C, Fuenmayor FJ. Influence of the mineral staggering on the elastic properties of the mineralized collagen fibril in lamellar bone. J. Mech. Behav. Biomed. Mater. 2014;42: 243-256.
23. Reznikov N, Shahar R, Weiner S. Bone hierarchical structure in three dimensions. Acta Biomaterialia, 2014; 10(9): 3815-3826.
24. Liu Y, Chen B, Yin D. Effects of arrangement direction and shape of osteocyte lacunae on resisting impact and micro-damage of osteon. J Mater Sci: Mater Med, 2017; 28: 38.
25. Liu Y, Li A, Chen B. Effects of Structure Characteristics of Osteocyte Lacunae on Squeeze Damage Resistance of Osteons. Cells Tissues Organs, 2019; 208:142–147.
26. Choi HY, Chang FK. A model for predicting damage in graphite/epoxy laminated composites from low-velocity point impact. J Compos Mater, 1992;26(14): 2134-2169.
27. Li S, Thouless MD, Wass AM. Use of mode-I cohesive-zone models to describe the fracture of an adhesivley-bonded polymer-matrix composite. Compos Sci Technol, 2005; 65(2): 281-293.
28. Hsshin Z. Failure criteria for unidirectional fiber composites. Journal of Applied Mechanics, 1980; 47(2): 329-334.

Tab.1-Models of multilayer fiber bionic composites

Bionic Models	Fiber laying mode
Orthogonal model(Sample90)	$[0/90]_{6s}$
Small helix angle model(Sample15)	[0/15/30⋯/165]
Medium helix angle model(Sample30)	$[0/30/60\cdots/150]_{2s}$
Large helix angle model(Sample60)	$[0/60/120]_{4s}$

Tab.2-Characteristic parameters of composite material

Material characteristics	**Value**	**Material characteristics**	**Value**
Densityρ/(kg/m3)	1830	Longitudinal shear modulusG_{12}/GPa	3.1
Longitudinal modulusE_{11}/GPa	40.51	Transverse shear modulusG_{23}/GPa	2.9
Transverse modulusE_{22}/GPa	13.96	Longitudinal shear strengthS_{12}/MPa	69
Poisson's ratiov_{12}	0.22	Transverse shear strengthS_{23}/MPa	38
Longitudinal tensile strengthX_t/MPa	783.3	Longitudinal critical energy release rate$G_{cr,L}$/(kN·m^{-1})	40
Longitudinal compression strengthX_c/MPa	298	Transverse critical energy release rate$G_{cr,T}$/(kN·m^{-1})	0.3
Transverse tensile strengthY_t/MPa	64	Transverse compressive strengthY_c/MPa	124

Tab.3-Material stiffness degradation criterion

Damage mode	Degradation criteria
Matrix tensile failure($\sigma_{22}\geq 0$)	$Q_0=0.2Q(Q=E_{22}, G_{23}, v_{12})$
Matrix compression failure($\sigma_{22}<0$)	$Q_0=0.4Q(Q=E_{22}, G_{23}, v_{12})$
Fiber tensile failure($\sigma_{11}\geq 0$)	$Q_0=0.07Q(Q=E_{11}, G_{23}, v_{12})$
Fiber compression failure($\sigma_{11}<0$)	$Q_0=0.2Q(Q=E_{11}, G_{23}, v_{12})$

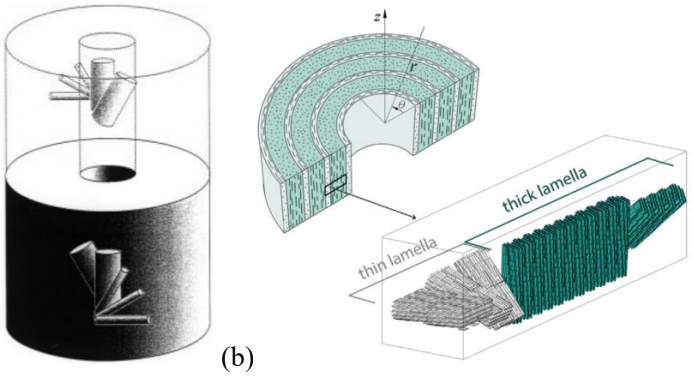

(b)

Fig. 1 Microstructure schematic diagram of fiber arrangement in osteon, (a) The direction of fibers in adjacent sub-lamella, (b) structure and directions of thin and thick lamellae

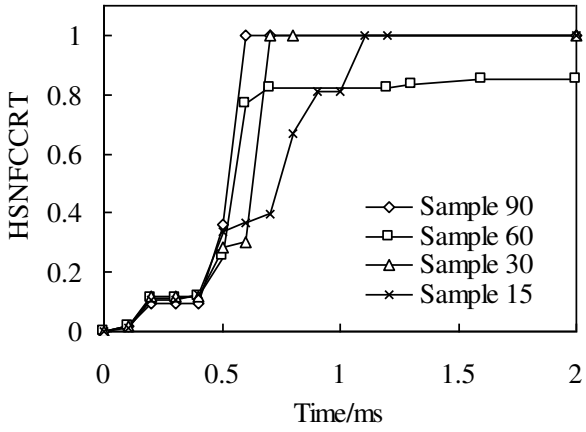

Fig. 2 The relationship of fiber compression failure and impact time history

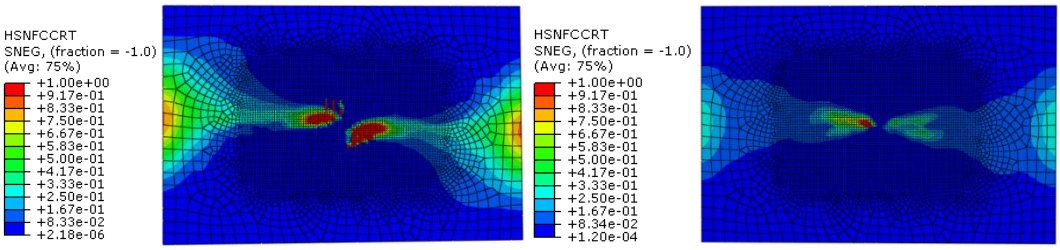

Sample 15 Sample 30

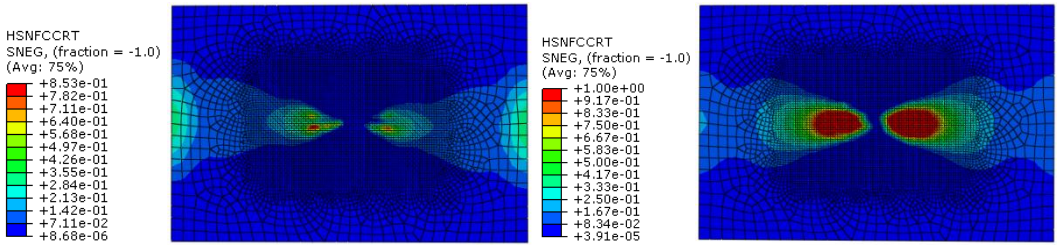

Sample 60 Sample 90

Fig.3 The fiber compression failure distribution when the impact energy is 20J

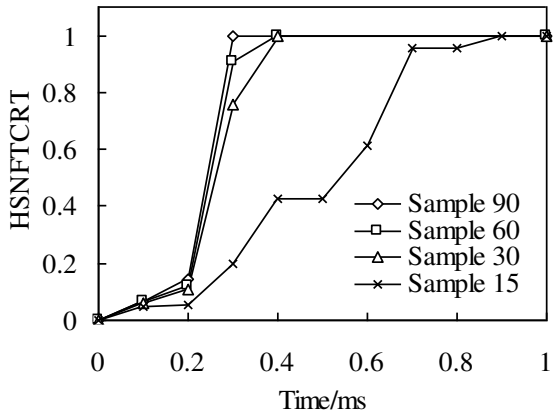

Fig. 4 The relationship of fiber tensile failure and impact time history

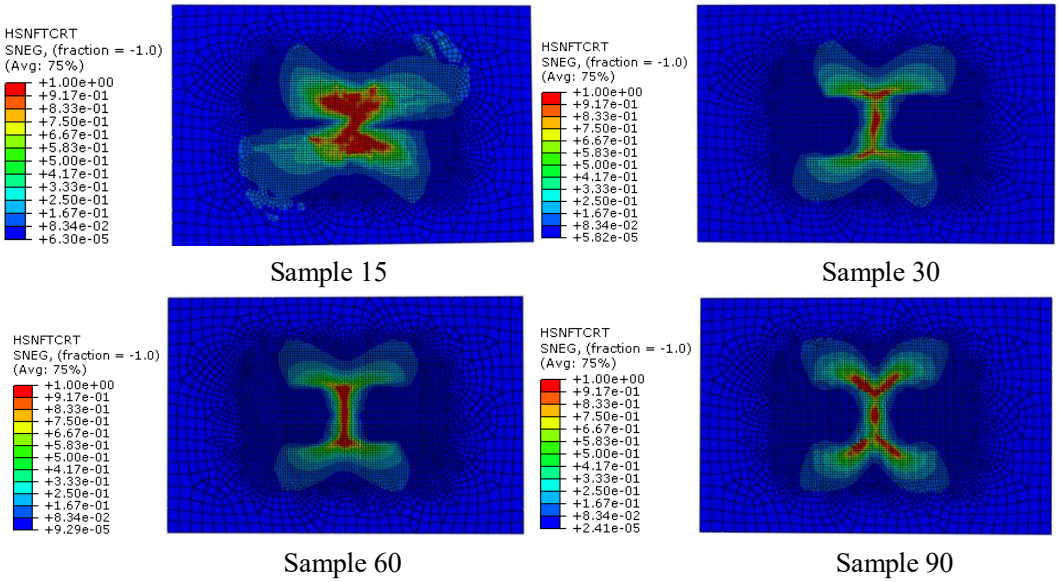

Fig. 5 The fiber tensile failure distribution when the impact energy is 20J

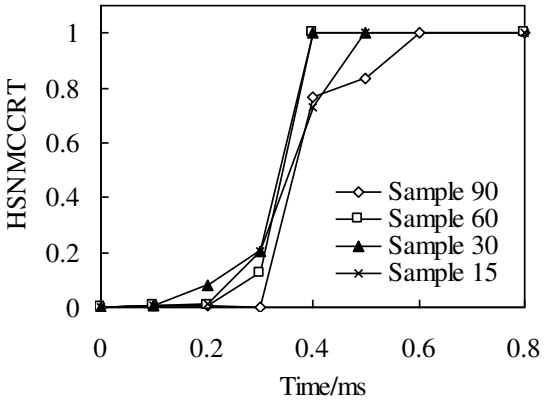

Fig. 6 The relationships of matrix compression failure and impact time history

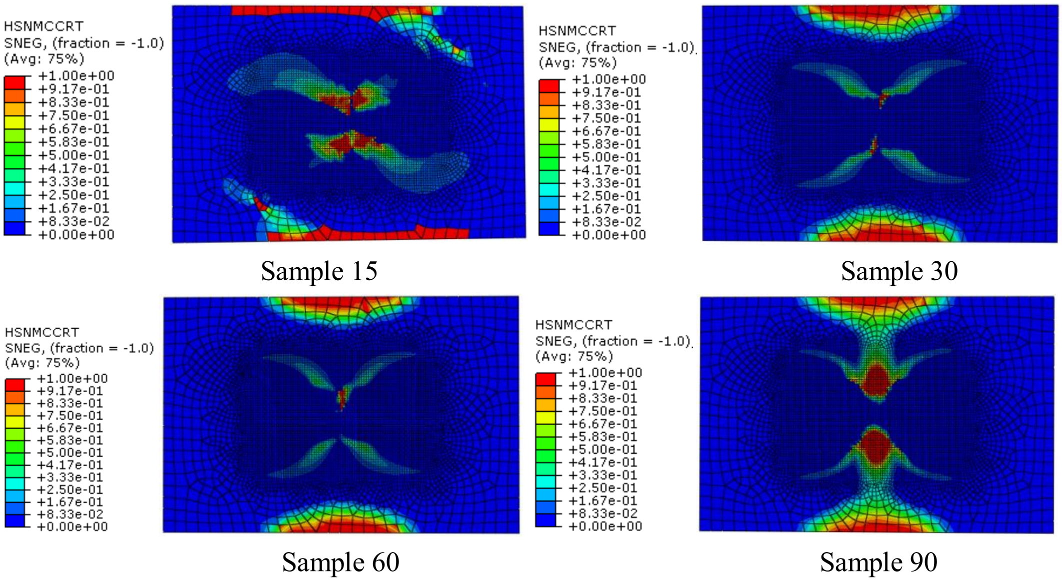

Fig. 7 The matrix compression failure distribution when the impact energy is 20J

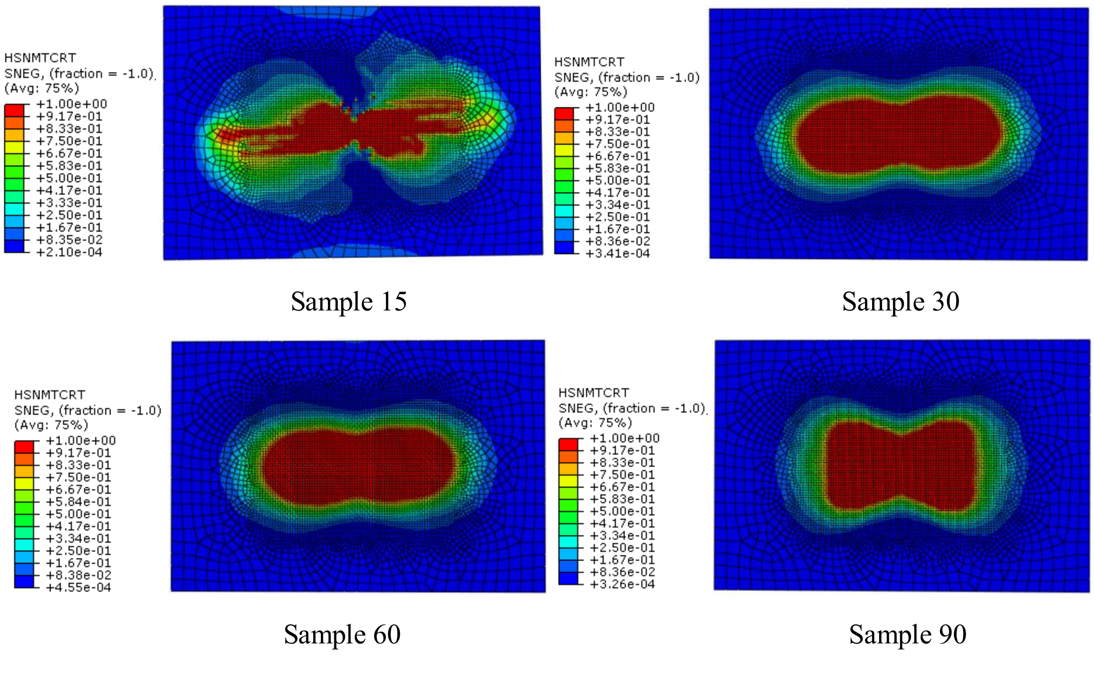

Fig. 8 The distribution of tensile failure of matrix when the impact energy is 20J

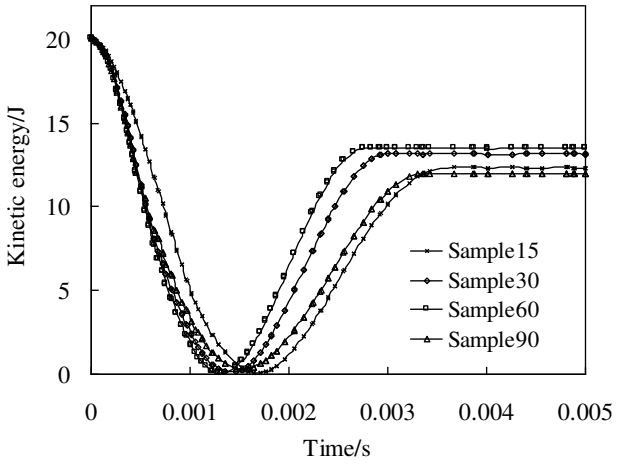

Fig. 9 The change history of kinetic energy of the four models when the impact energy is 20J

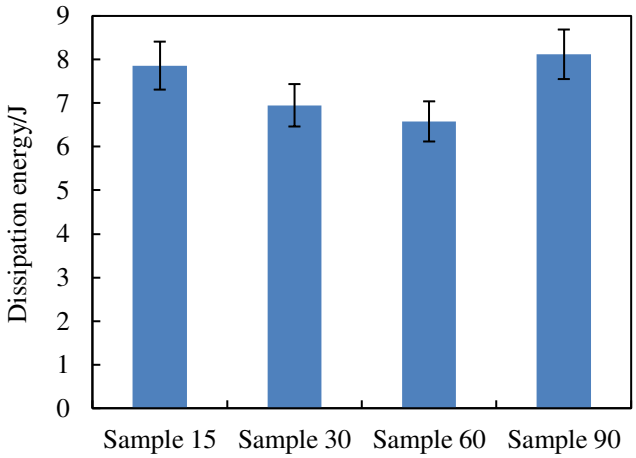

Fig. 10 The dissipated energy of the four different models when the impact energy is 20J

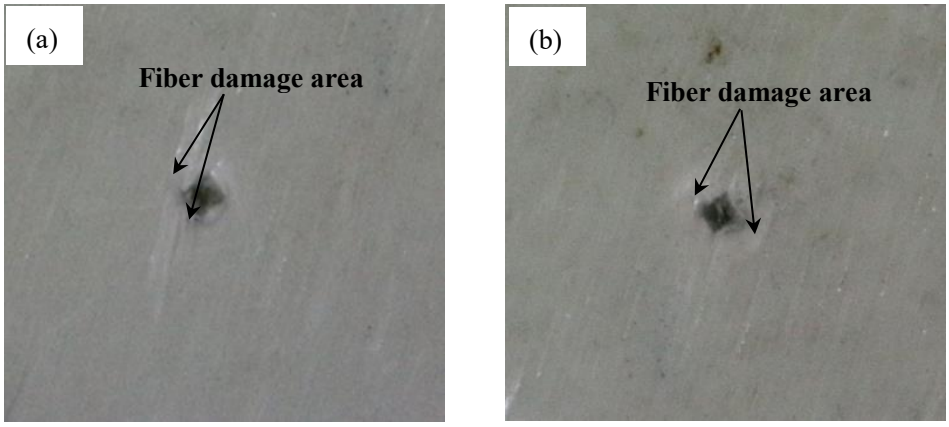

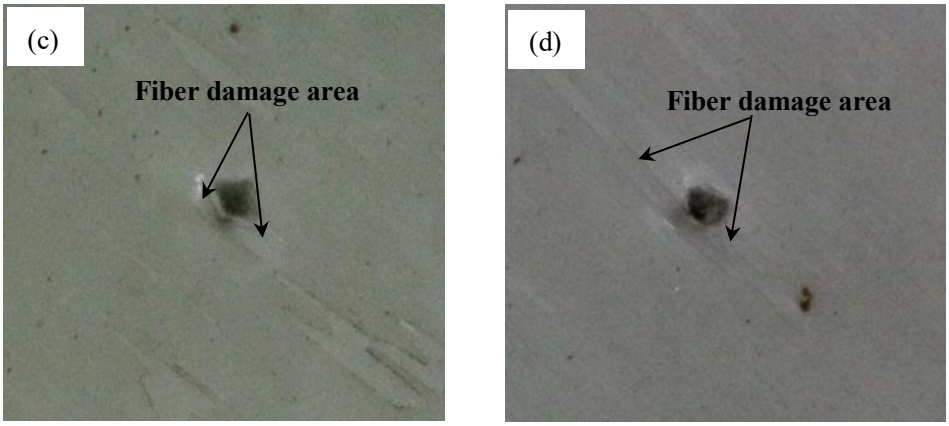

Fig.11 Damage to the specimens. (a)15°, (b)30°, (c)60°, (b)90°

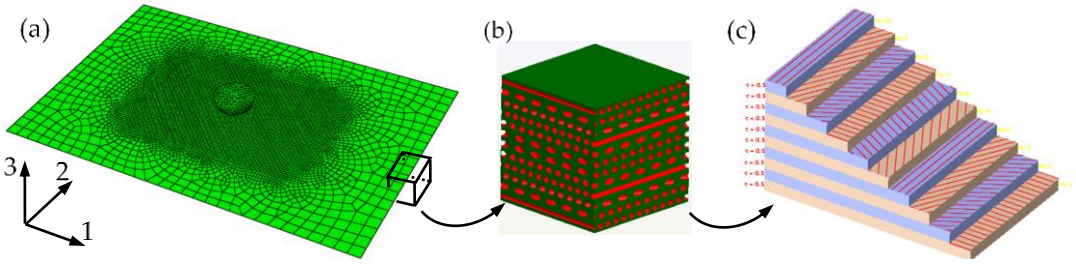

Fig. 12 FE model of bionic composite. (a) Finite element model for impact analysis of periodic helicoidal bionic structure, (b) local enlarged view of the model (red represents fiber and green represents matrix), (c) direction of fiber arrangement of composite

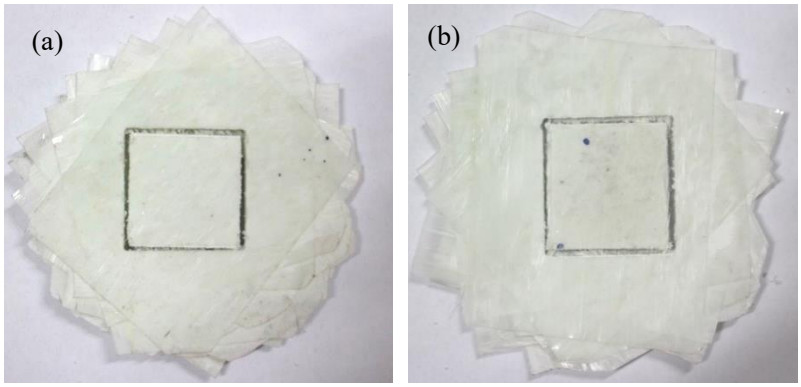

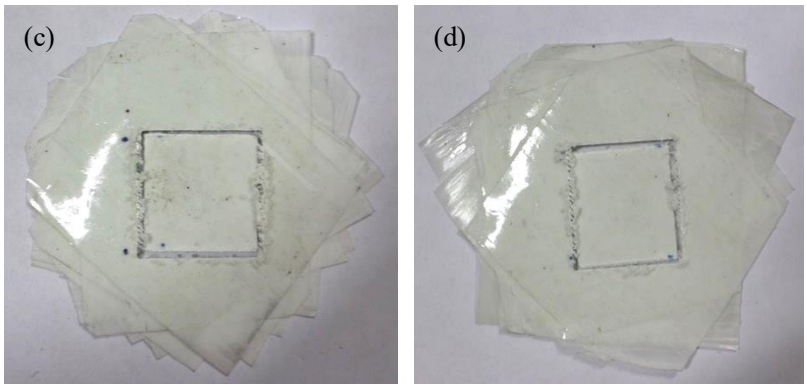

Fig.13 Biomimetic composite laminates with different spiral angles. (a) 15°, (b) 30°, (c) 60°, (b) 90°

Figures

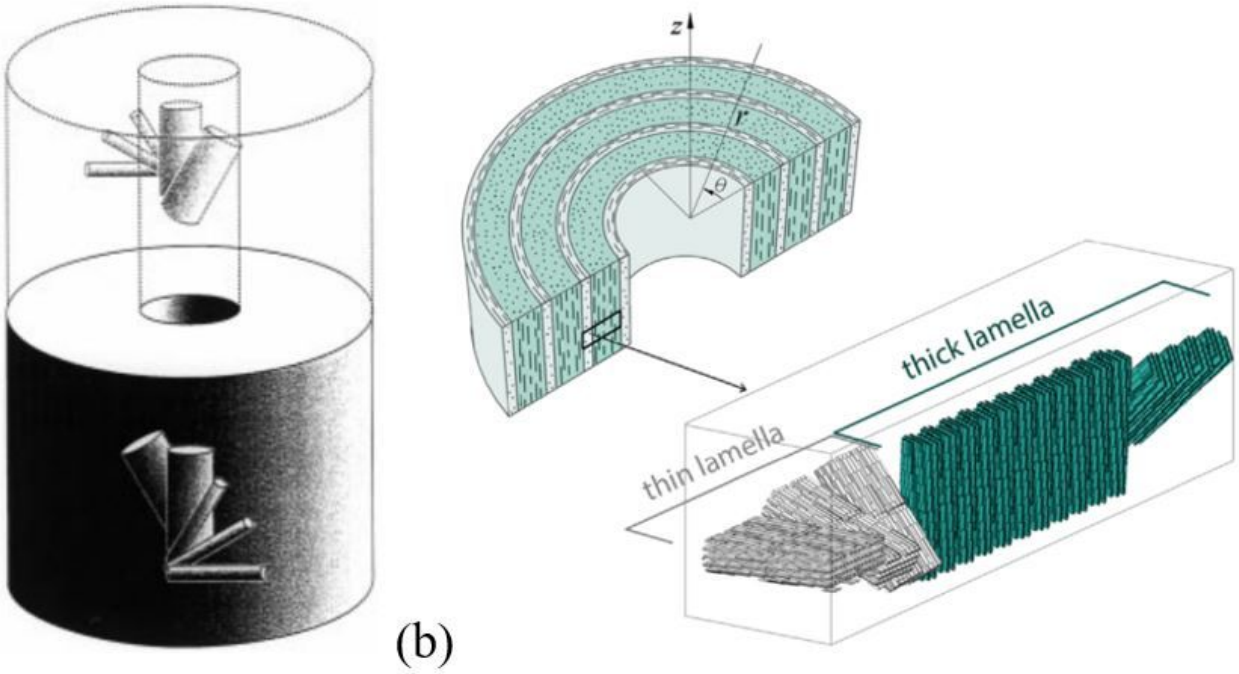

Figure 1

Microstructure schematic diagram of fiber arrangement in osteon, (a) The direction of fibers in adjacent sub-lamella, (b) structure and directions of thin and thick lamellae

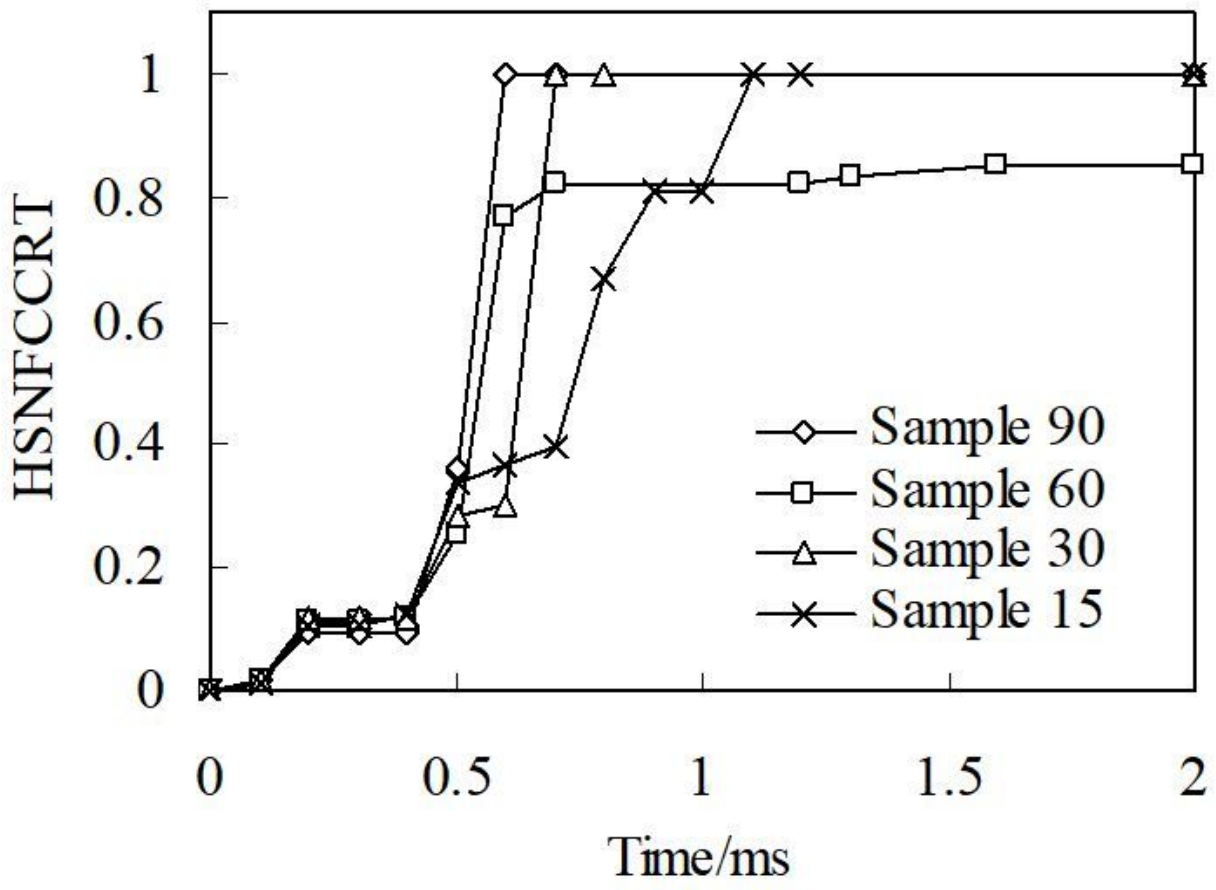

Figure 2

The relationship of fiber compression failure and impact time history

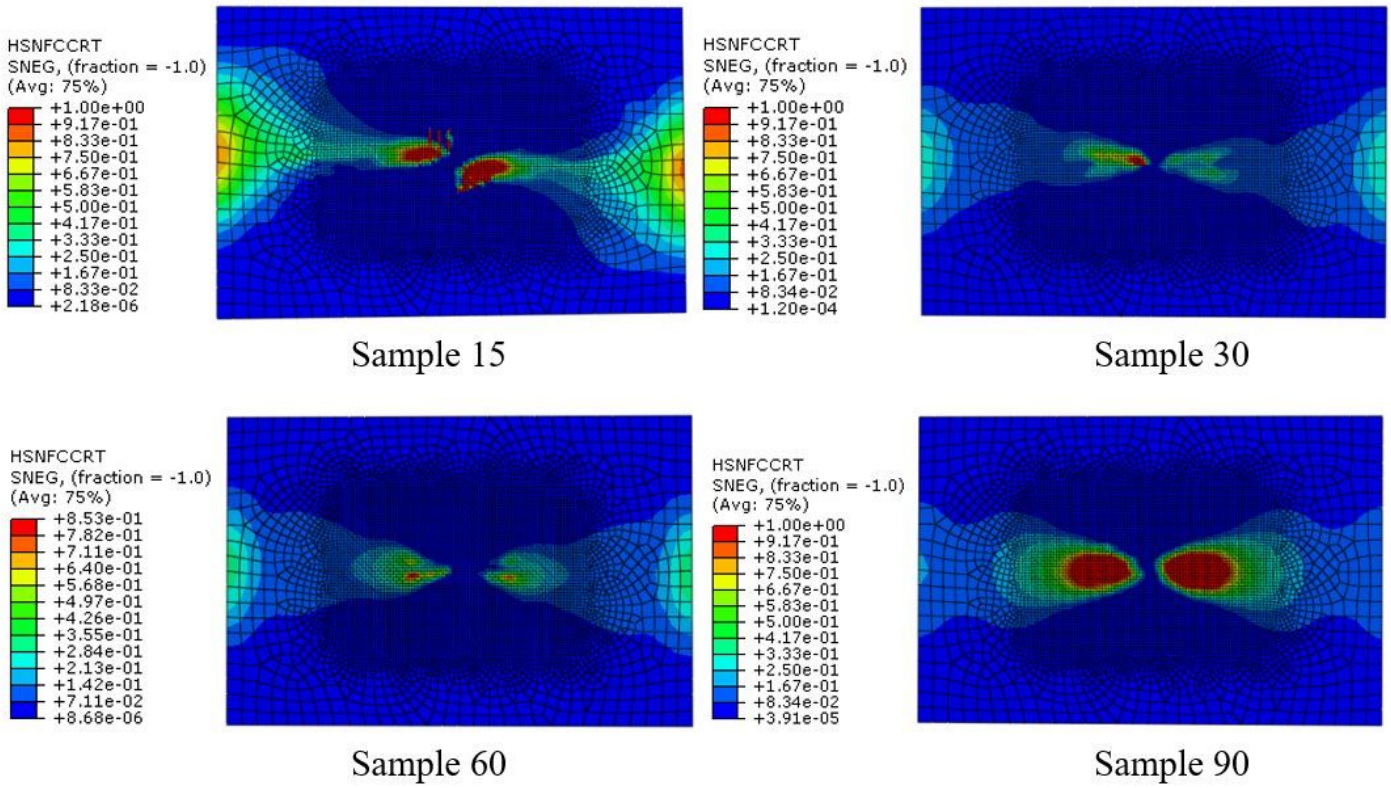

Figure 3

The fiber compression failure distribution when the impact energy is 20J

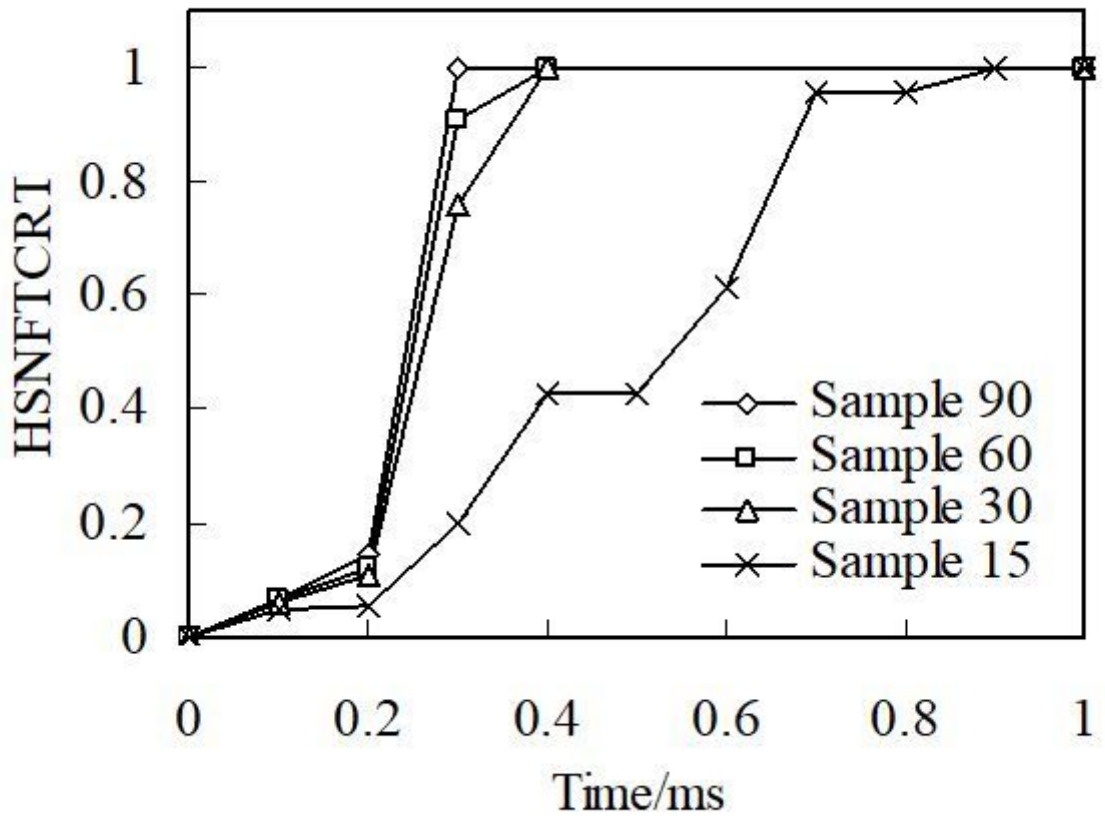

Figure 4

The relationship of fiber tensile failure and impact time history

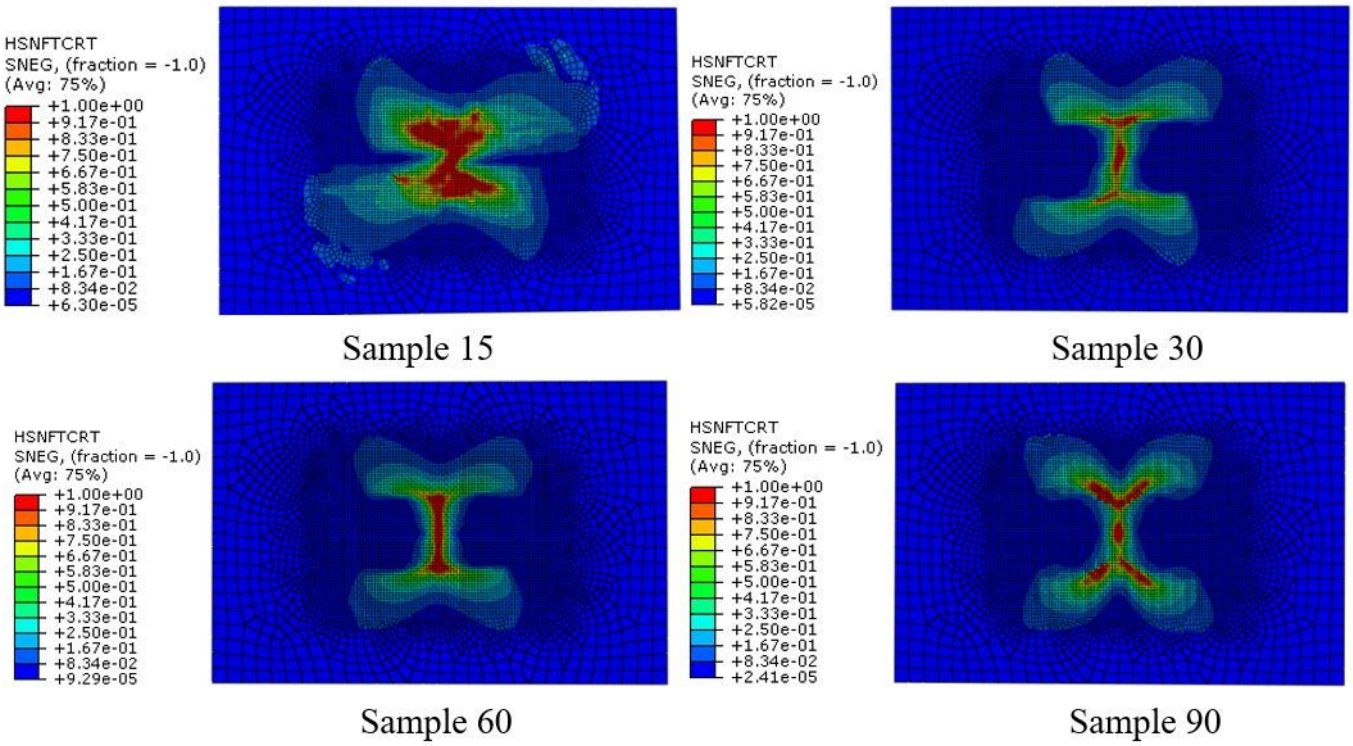

Figure 5

The fiber tensile failure distribution when the impact energy is 20J

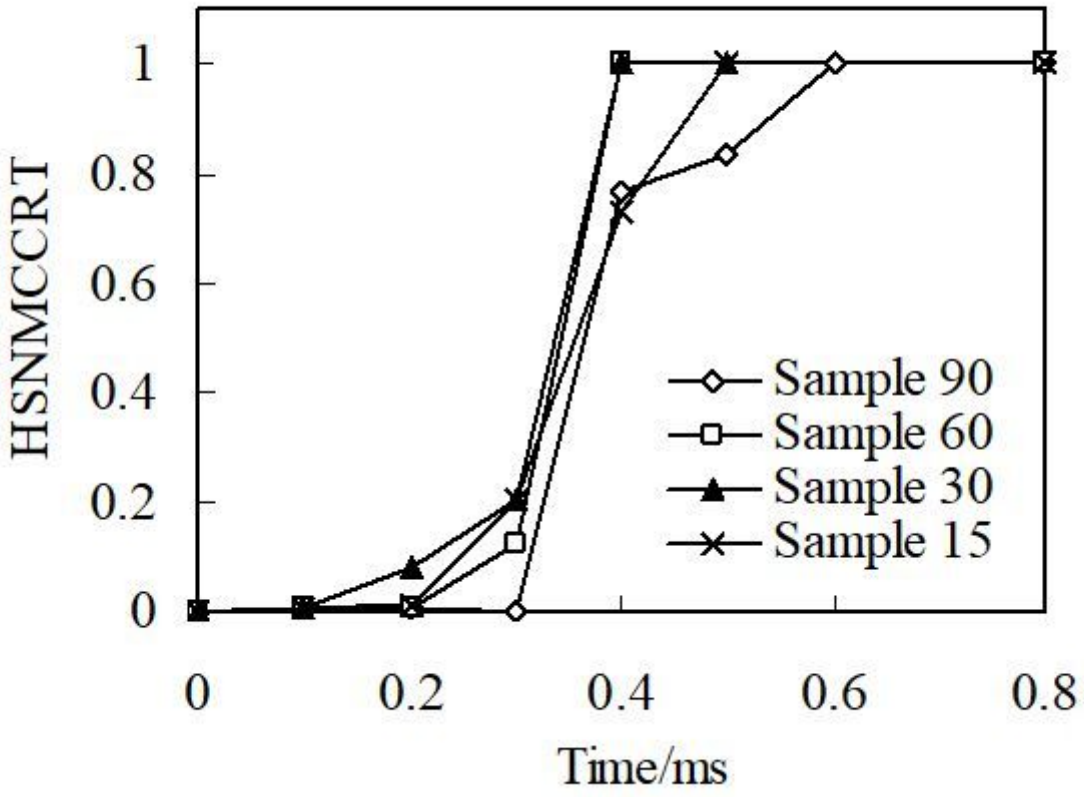

Figure 6

The relationships of matrix compression failure and impact time history

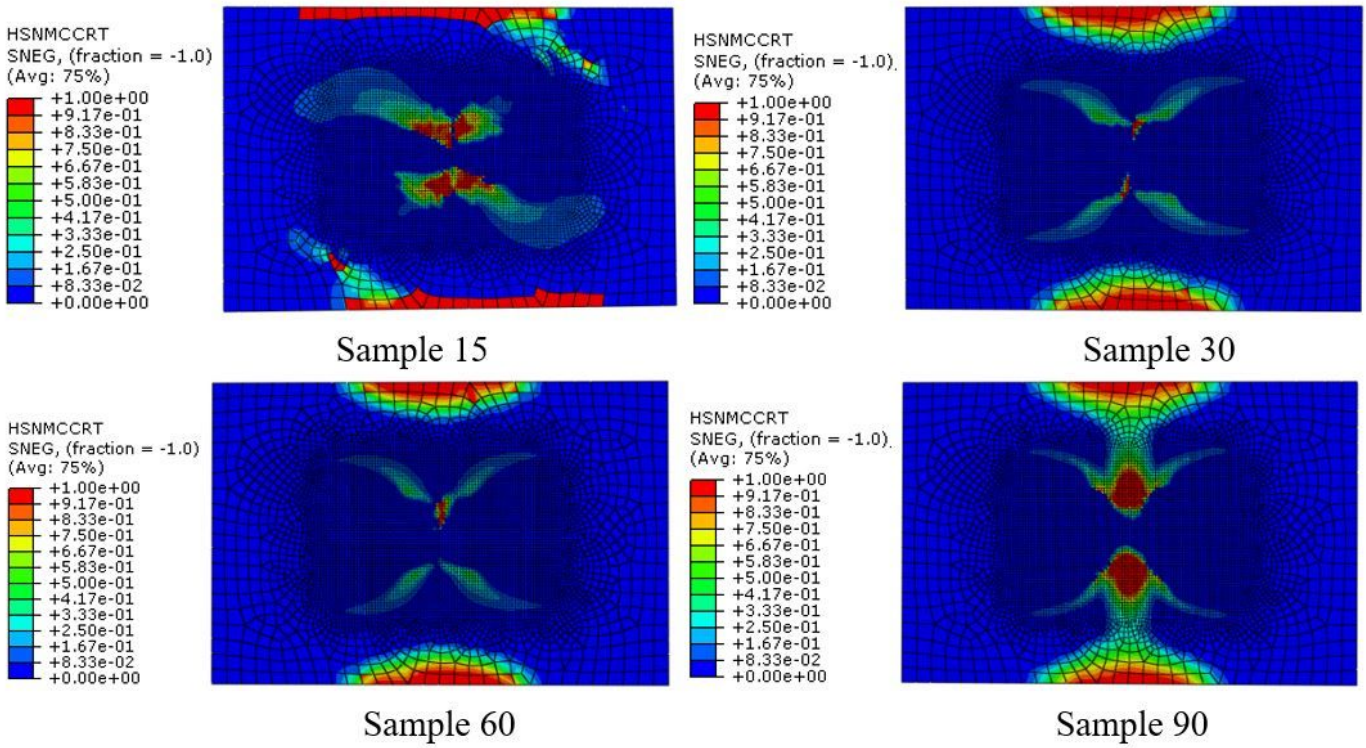

Figure 7

The matrix compression failure distribution when the impact energy is 20J

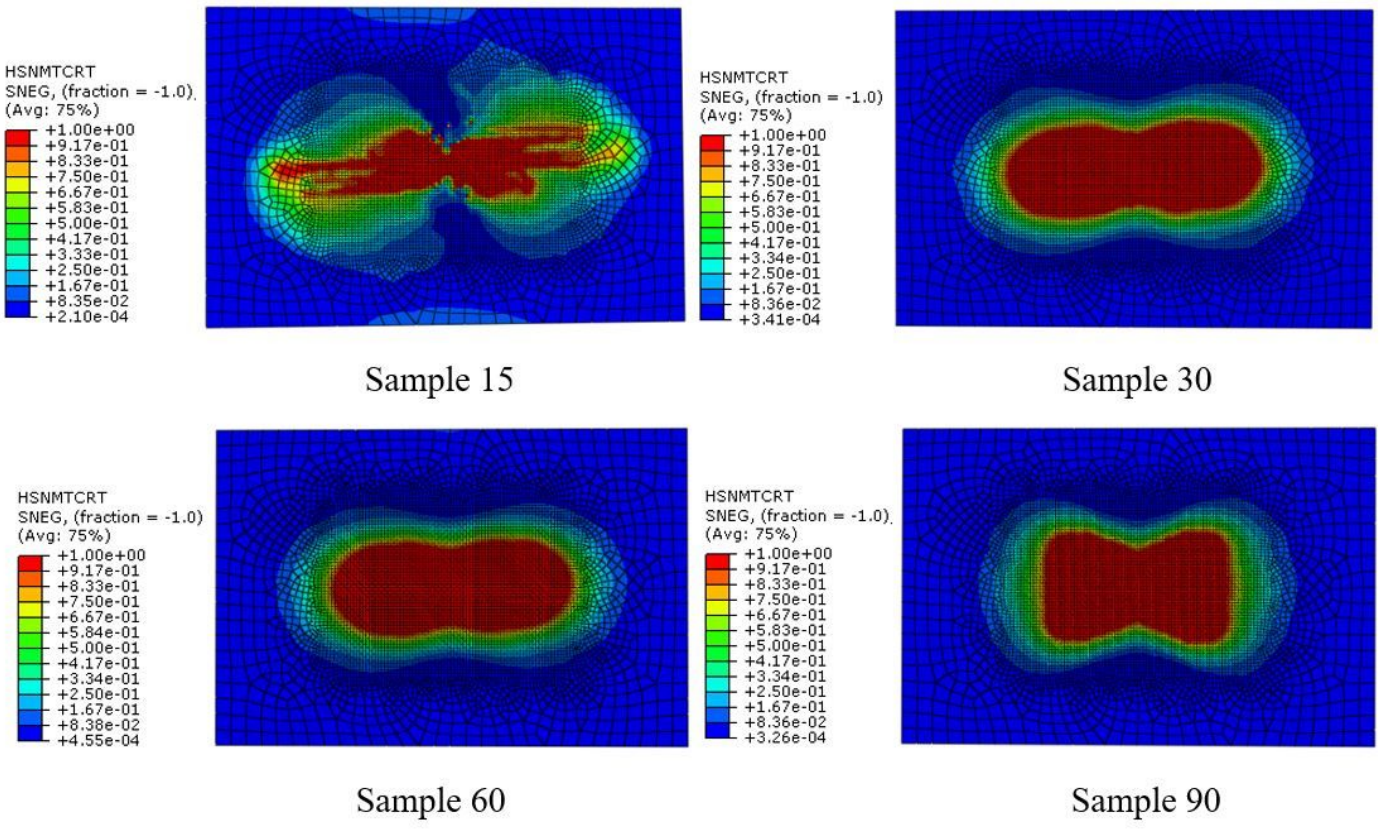

Figure 8

The distribution of tensile failure of matrix when the impact energy is 20J

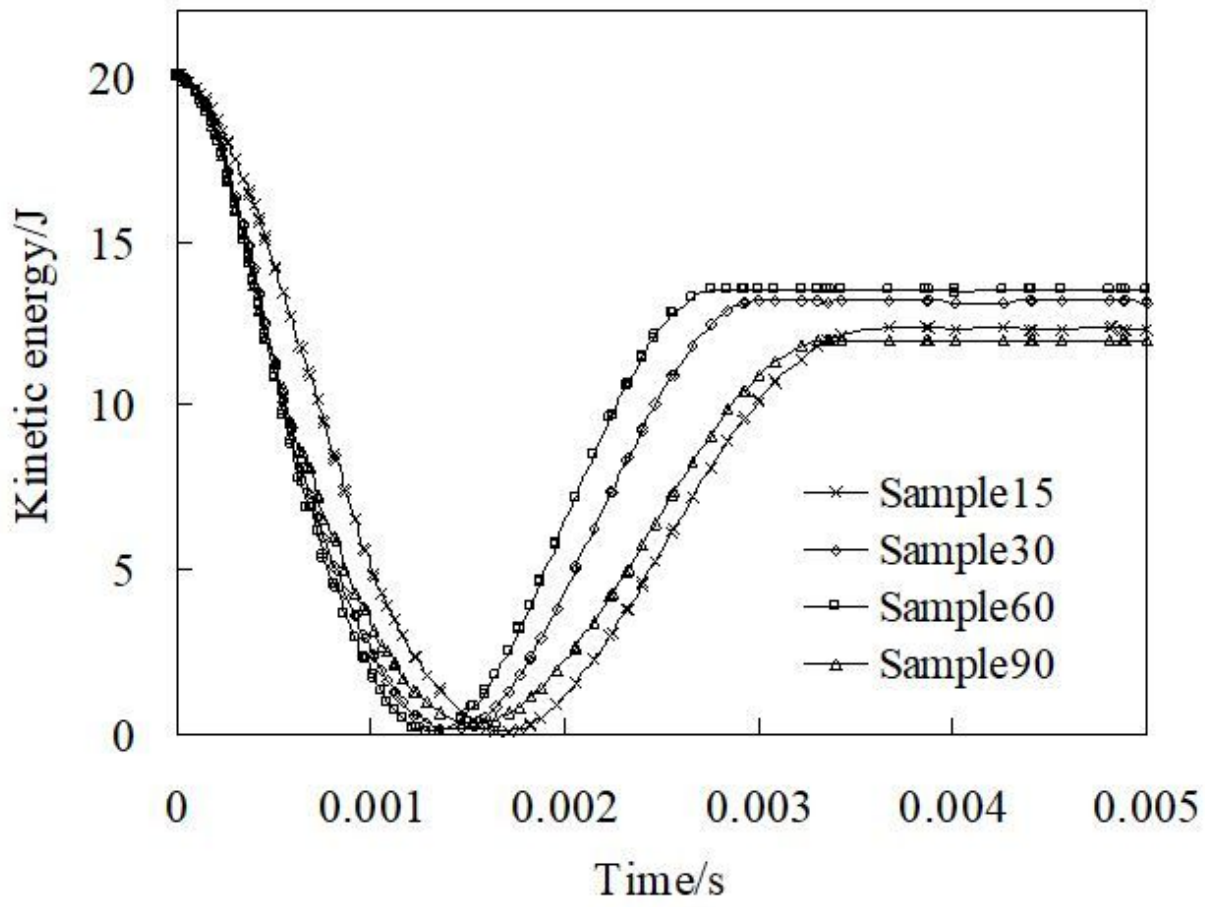

Figure 9

The change history of kinetic energy of the four models when the impact energy is 20J

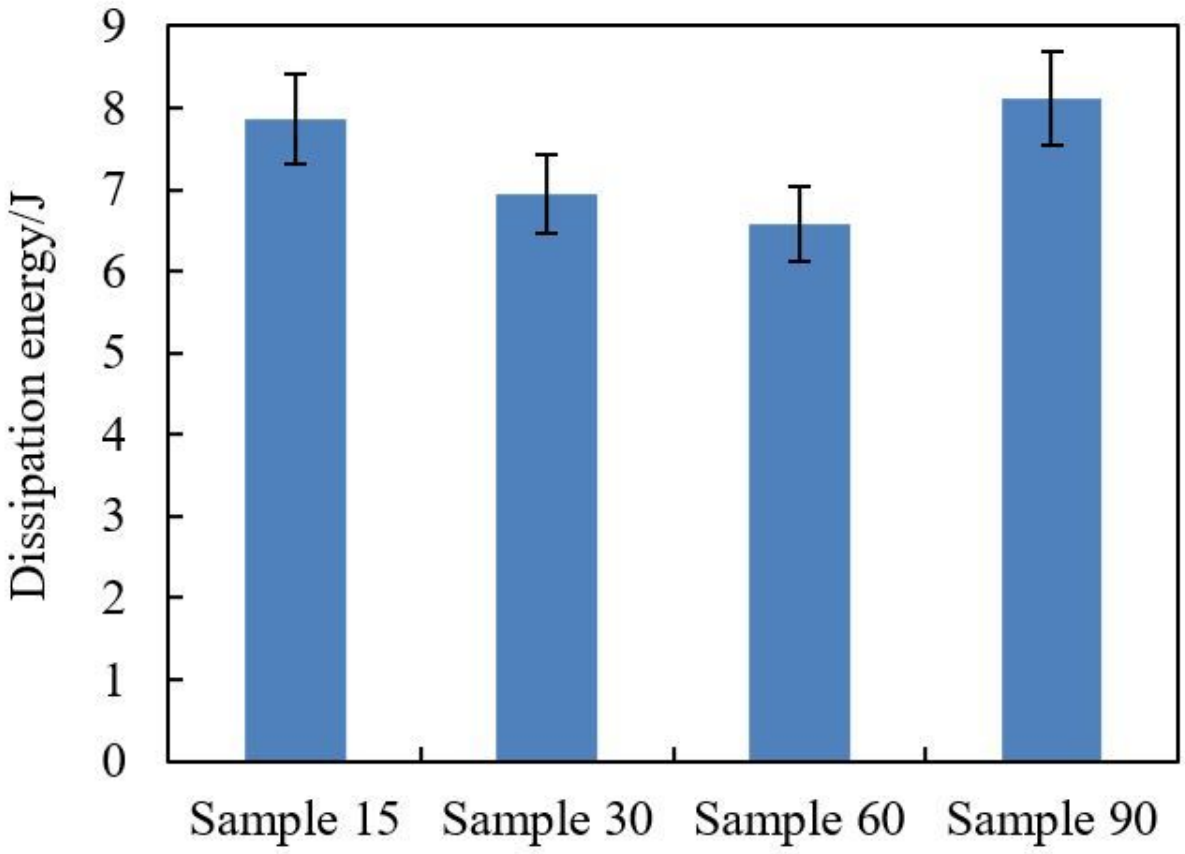

Figure 10

The dissipated energy of the four different models when the impact energy is 20J

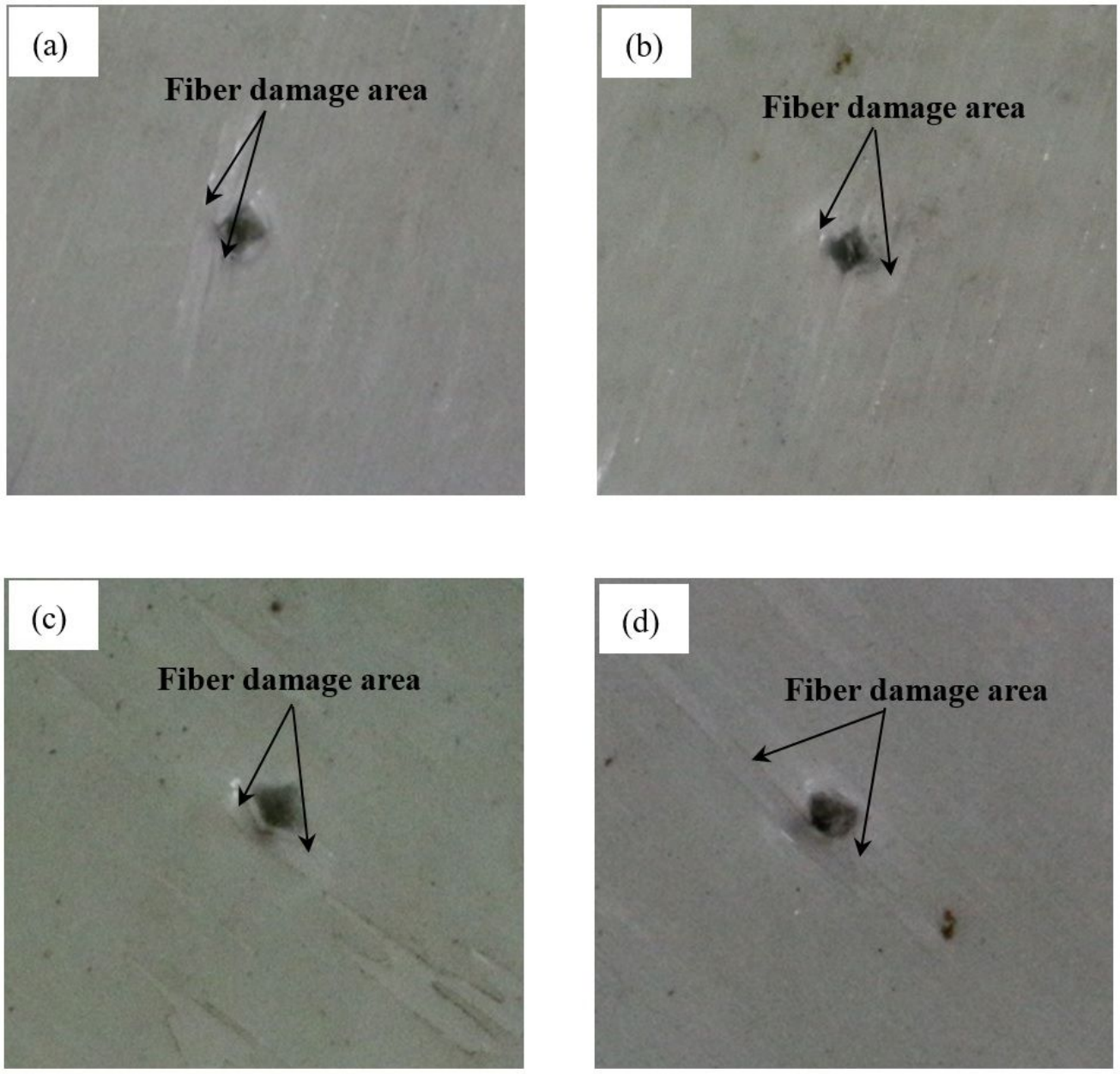

Figure 11

Damage to the specimens. (a)15°, (b)30°, (c)60°, (b)90°

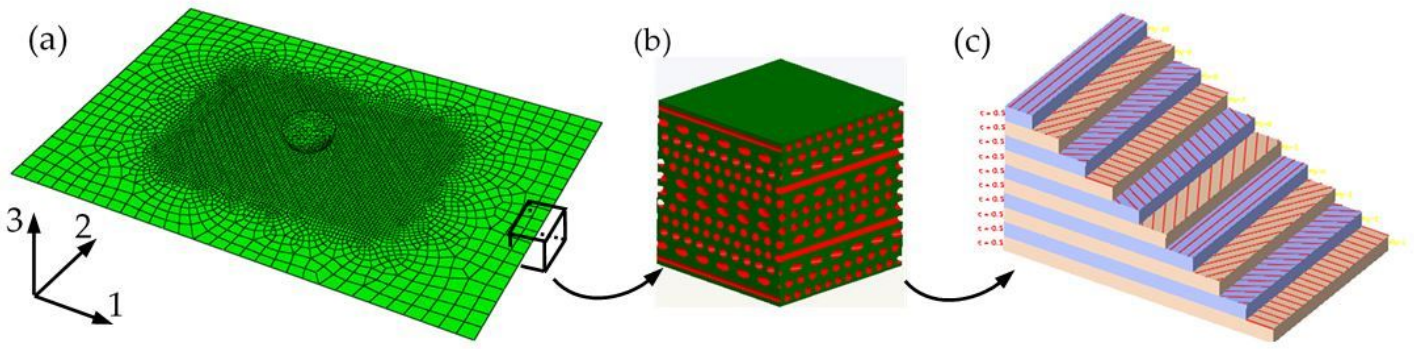

Figure 12

FE model of bionic composite. (a) Finite element model for impact analysis of periodic helicoidal bionic structure, (b) local enlarged view of the model (red represents fiber and green represents matrix), (c) direction of fiber arrangement of composite

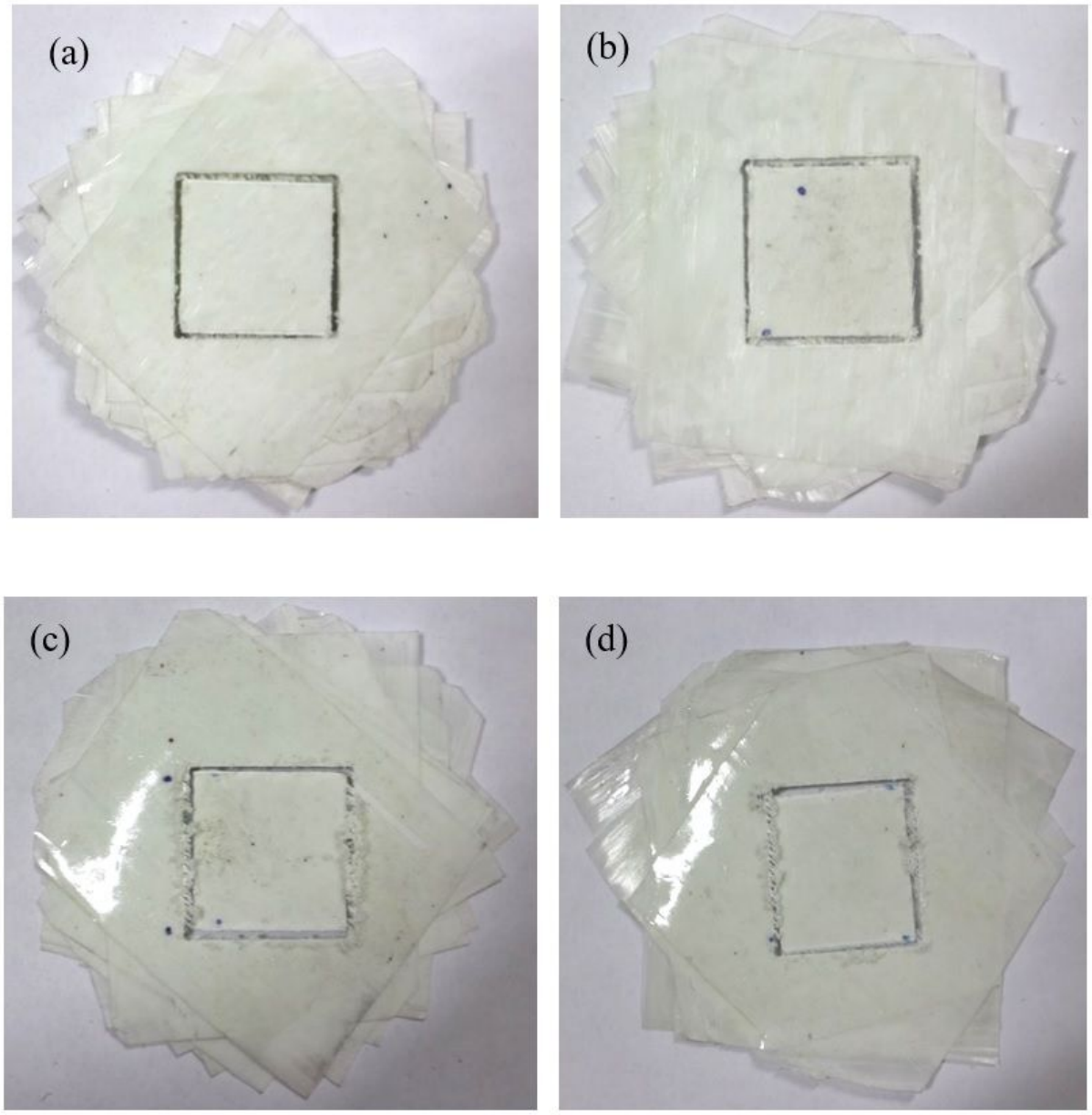

Figure 13

Biomimetic composite laminates with different spiral angles. (a) 15°, (b) 30°, (c) 60°, (b) 90°